Ecotoxicology and Environmental Safety 183 (2019) 109496

Contents lists available at ScienceDirect

Ecotoxicology and Environmental Safety

journal homepage: www.elsevier.com/locate/ecoenv

Iron (III) oxide nanoparticles alleviate arsenic induced stunting in *Vigna radiata*

Nisha Shabnam[a,*], Minsoo Kim[a], Hyunook Kim[a,**]

[a] Department of Environmental Engineering, University of Seoul, Seoul, Republic of Korea

ARTICLE INFO

Keywords:
Arsenic
Fe_2O_3 nanoparticles
Oxidative stress
Vigna radiata

ABSTRACT

Iron nanoparticles (NPs) are widely used for the removal of arsenic from water. In this study, we evaluated the interaction between arsenate (AsO_4^{3-}) and Fe_2O_3-NPs on early seedling growth of *Vigna radiata*. Seedlings were raised in AsO_4^{3-} and Fe_2O_3-NPs, alone and in combination. While Fe_2O_3-NPs slightly promoted seedling growth, AsO_4^{3-} reduced seedling growth drastically. AsO_4^{3-}-induced decline in the seedling growth was recovered by Fe_2O_3-NPs. In contrast, equivalent concentrations of $FeCl_3$, alone and together with AsO_4^{3-}, inhibited seed germination completely. Lower arsenic content in seedlings raised in the presence of Fe_2O_3-NPs indicated that Fe_2O_3-NPs restricted arsenic uptake. Ability of Fe_2O_3-NPs to restrict the arsenic uptake of the seedlings was due to adsorption of AsO_4^{3-}, as revealed by transmission and scanning electron microscopy. Non-toxic levels of iron in seedlings were due to restriction of Fe_2O_3-NPs to root-surface. AsO_4^{3-} enhanced the ferric chelate reductase activity of root which was recovered by Fe_2O_3-NPs. The AsO_4^{3-}-induced oxidative stress, evident from high levels of proline, H_2O_2 and malondialdehyde, and lowered root oxidisability was ameliorated by Fe_2O_3-NPs. AsO_4^{3-}-induced enhancement in total antioxidant capacity, superoxide dismutase and catalase activity, and decline in guaiacol peroxidase activity were antagonized by Fe_2O_3-NPs. Our findings reveal that Fe_2O_3-NPs provide effective resistance/amelioration to arsenic toxicity by reducing arsenic availability to plants.

1. Introduction

Exclusive size-dependent properties of nanoparticles (NPs) over bulk material are beneficial for a wide range of applications which have affirmed their omnipresence in our lives. Among the metal NPs, Fe-based NPs hold special importance due to their magnetic properties. They find applications in industrial and domestic sectors ranging from healthcare, biomedical, energy, defense, construction, aerospace to textile, food, agriculture, and environmental bioremediation (Hokkanen et al., 2015; Ali et al., 2016). Fe-based NPs have been extensively used to decontaminate polluted water and are of interest to researchers working on wastewater treatment technologies (Xu et al., 2012; Hokkanen et al., 2015). Fe-based NPs are used as (i) absorbent or immobilisation carriers; and/or (ii) photocatalysts for conversion of pollutant to less/non-toxic forms (Xu et al., 2012). The target pollutants for Fe-based NPs include chlorinated compounds, inorganic ions, explosives, pesticides and toxic metals (Bezbaruah et al., 2009; Crane and Scott, 2012). Especially, they have been successfully applied for the removal of toxic elements including arsenic (Jang et al., 2008; Xu et al., 2012; Zou et al., 2016).

Arsenic contamination of soil and water is a widespread problem for its negative impact on living organisms human health. Excess arsenic levels in the environment can be a result of both natural and anthropogenic activities ranging from volcanic emissions, mineral weathering and leachate from metal oxide deposits to mining wastes, petroleum refining, agricultural chemicals, wood preservatives, ceramic manufacturing, gold mining, combustion of fossil fuels, etc. (Lenoble et al., 2005; Hokkanen et al., 2015). Apart from the contaminated soils, tube well water used for irrigation, and deposition of particulate matter also expose plants to arsenic (Meharg, 2004; Hu et al., 2012). Arsenic is a

Abbreviations: CAT, catalase; DTT, dithiothreitol; DPPH, 2,2-diphenyl-1-picrylhydrazyl; EDTA, ethylene diamine tetra acetic acid; EDS, energy dispersive spectroscopy; FCR, ferric chelate reductase; GPX, guaiacol peroxidase; MES, 2-(N-morpholino)ethanesfulfonic acid; NP, nanoparticle; NADP+, oxidized nicotinamide adenine dinucleotide (phosphate); NADPH, reduced nicotinamide adenine dinucleotide (phosphate); PVP, polyvinylpyrrolidone; SEM, scanning electron microscope; SOD, superoxide dismutase; TCA, trichloroacetic acid; TEM, Transmission electron microscope; Tris, tris-(hydroxymethyl)-aminomethane; TTC, triphenyl tetrazolium chloride

* Corresponding author.
** Corresponding author.
E-mail addresses: shabnam251@gmail.com, shabnam251@uos.ac.kr (N. Shabnam), kcmpower@naver.com (M. Kim), h_kim@uos.ac.kr (H. Kim).

https://doi.org/10.1016/j.ecoenv.2019.109496
Received 11 April 2019; Received in revised form 26 July 2019; Accepted 29 July 2019
Available online 31 July 2019

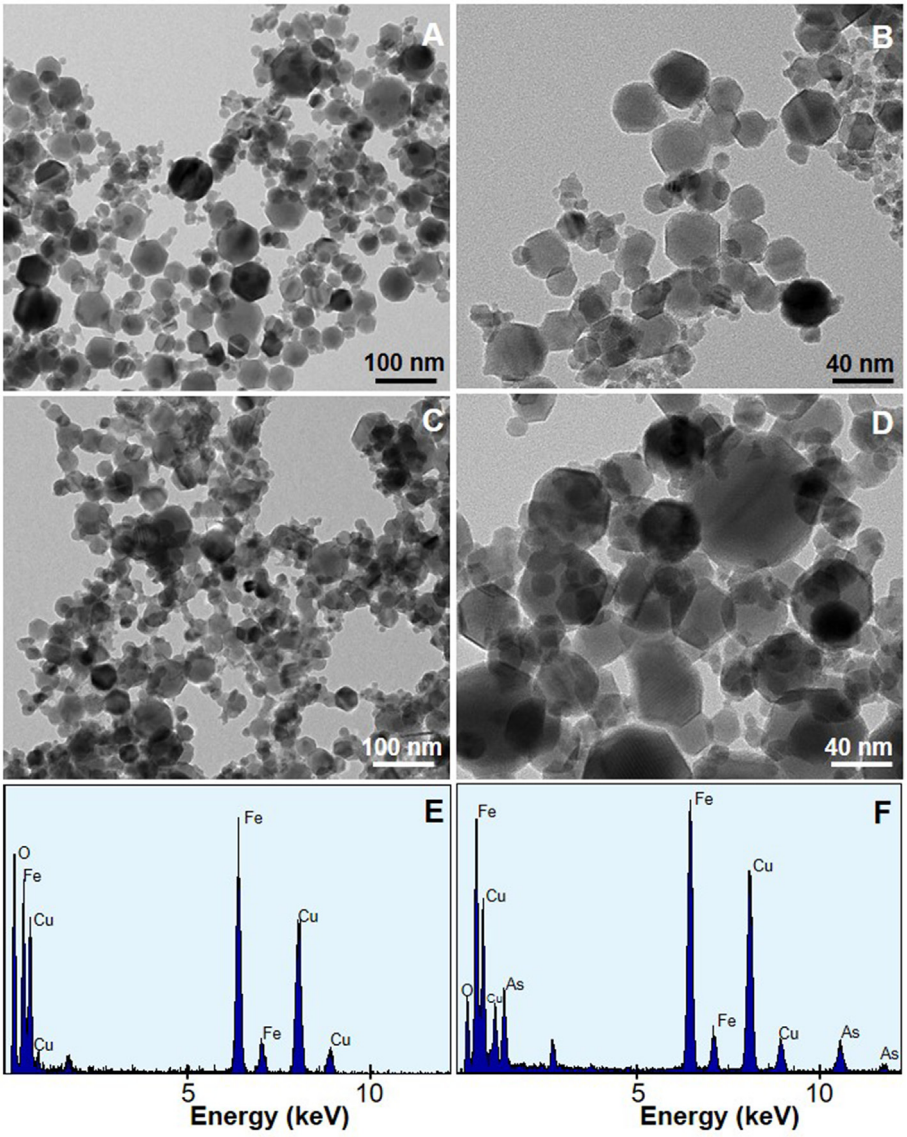

Fig. 1. TEM pictures (A–D) and EDS (E,F) of Fe_2O_3-NPs in absence (A,B,E) and presence (C,D,F) of AsO_4^{3-} to which *Vigna radiata* seedlings were exposed.

non-essential and highly toxic element for plant growth and hampers agricultural productivity (Hartley and Lepp, 2008; Duncan et al., 2017). Toxicity of arsenic depends on its bioavailability to plants which is governed by various factors in soil like redox potential, pH and microbial activity (Singh et al., 2009; Farooq et al., 2016; Praveen et al., 2018). Two inorganic forms of arsenic, i.e., arsenite (AsO_3^{3-}) and arsenate (AsO_4^{3-}) prevail in anaerobic and aerobic soils, respectively; AsO_3^{3-} is more toxic than AsO_4^{3-} (Singh et al., 2009; Praveen et al., 2018). Several studies have shown the presence of arsenic in plants and their grains thus serving a dietary exposure of a large population to arsenic (Meharg, 2004; Duncan et al., 2017).

Numerous efforts have been made to decontaminate arsenic polluted soils to prevent its transfer into the food chain. Stabilisation of contaminants by addition of soil amendments is a popular in-situ approach, wherein the amendment may bind, absorb/adsorb or co-precipitate the contaminant (Hartley and Lepp, 2008). Among various amendments exploited to reduce arsenic bioavailability to plants, Fe-based technologies remain very popular (Mench et al., 2006; Cundy et al., 2008). These include use of Fe-oxides to reduce the bioavailability of arsenic and other contaminants to plants at polluted sites (Hartley and Lepp, 2008; Cundy et al., 2008). In fact, sorption of dissolved arsenic is positively correlated with soil Fe-oxides content (Warren et al., 2003). Another alternative is the use of $FeSO_4$ which forms Fe-oxides that later get precipitated down (Hartley and Lepp, 2008; Cundy et al., 2008). Fe(0) has been studied in cutting down the mobility and availability of arsenic along with other heavy metals in contaminated soils without altering the soil enzyme activities (Kumpiene et al., 2006). Although the above treatments yielded positive results in reducing the bioavailability of arsenic from soils, they were reported to exert negative effects on the vegetation (Hartley and Lepp, 2008). Effective roles of Fe-based NPs in removal of arsenic from wastewater/groundwater have been proved beyond any doubt, however, the same has not been studied in soil so far with the exception of a study by Shipley et al. (2011) who reported removal of arsenic from soil by Fe-NPs through column studies.

It is possible that Fe-based NPs will soon be used to remediate arsenic-contaminated soils, therefore there is a need to understand the effect that Fe-based NPs might have on vegetation in the presence of arsenic. The aim of the present study was to assess the ability of Fe-NPs to reduce the deleterious effect of arsenic on early seedling growth of Mung bean (*Vigna radiata* (L.)R.Wilczek.) Mung bean has an annual production of ~3 million tonnes in the world (War et al., 2017). The

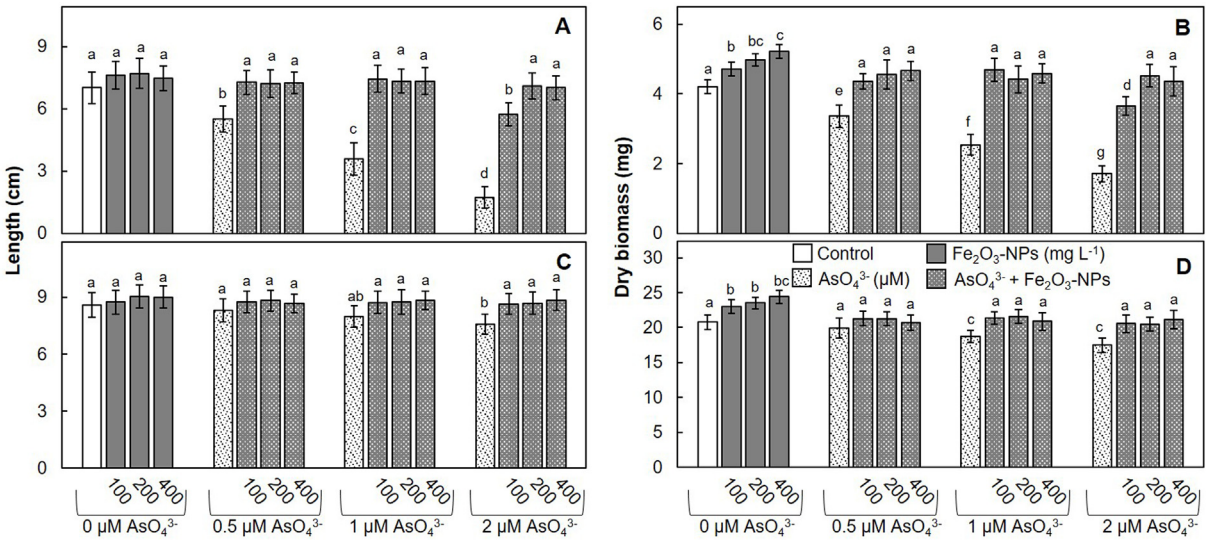

Fig. 2. Impact of Fe_2O_3-NPs on AsO_4^{3-}-induced changes in growth of *Vigna radiata* seedlings. Length (A,C) and fresh weight (B,D) of root (A,B) and shoot (C,D). Vertical lines on bars represent standard error. Values designated by different small letters between control and other treatments are significantly different at $P < 0.05$.

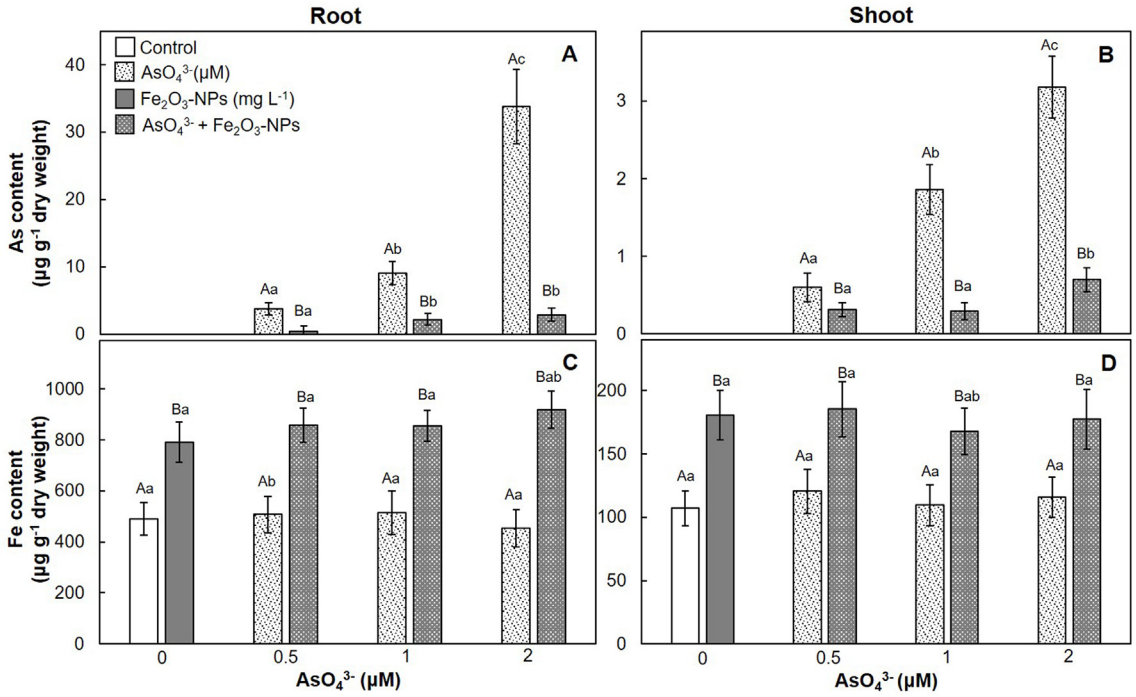

Fig. 3. Arsenic (A,B) and iron (C,D) content in roots (A,C) and shoots (B,D) of *Vigna radiata* seedlings raised in AsO_4^{3-} in absence and presence of Fe_2O_3-NPs. Vertical lines on bars represent standard error. Values designated by (i) different capital letters between AsO_4^{3-} and AsO_4^{3-} + Fe_2O_3-NPs treatments at a given AsO_4^{3-} concentration; and (ii) small letters between varying concentrations of AsO_4^{3-} and AsO_4^{3-} + Fe_2O_3-NPs treatments, are significantly different at $P < 0.05$.

high digestible protein content and the ability to grow well in drought and nitrogen deficient conditions, and improve the soil fertility, makes Mung bean an important crop in Asian region (War et al., 2017).

2. Materials and methods

2.1. Materials

Seeds of *V. radiata* (cv-SML-668) were purchased from the Indian Agricultural Research Institute, New Delhi, India. Fe_2O_3-NPs and sodium arsenate were bought from Sigma-Aldrich (St. Louis, MO, USA).

2.2. Methods

2.2.1. Seedling growth in presence of AsO_4^{3-} and Fe_2O_3-NPs

A stock solution of 1000 mg L^{-1} Fe_2O_3-NPs was prepared with distilled water and sonicated (60 min) before use. Sodium arsenate was used as a salt for AsO_4^{3-}. Varying concentrations of AsO_4^{3-} and Fe_2O_3-NPs were prepared in distilled water and autoclaved (pressure-15 kg cm^{-2}; temperature-121 °C) for 20 min. Mixtures of AsO_4^{3-} and Fe_2O_3-NPs were prepared with the respective autoclaved solutions in a laminar flow hood just before inoculation of seeds. Seeds of *V. radiata* were washed with detergent, rinsed with distilled water thrice and surface sterilized with 2% sodium hypochlorite for 3–5 min. Seeds were

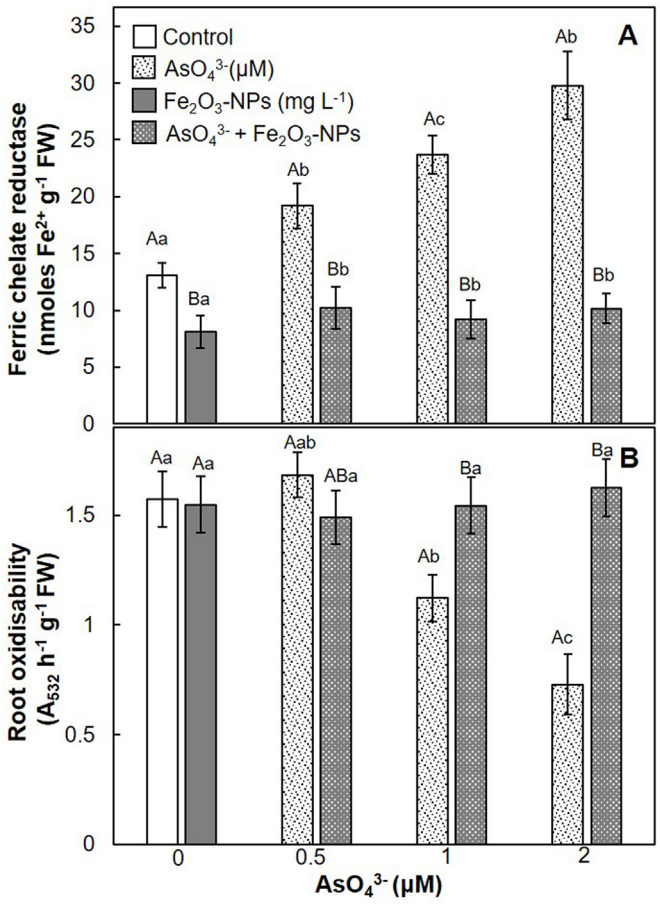

Fig. 4. Impact of Fe_2O_3-NPs on AsO_4^{3-}-induced changes in ferric chelate reductase activity (A) and oxidising capacity (B) of roots of *Vigna radiata* seedlings. Vertical lines on bars represent standard error. Values designated by (i) different capital letters between AsO_4^{3-} and AsO_4^{3-} + Fe_2O_3-NPs treatments at a given AsO_4^{3-} concentration; and (ii) small letters between varying concentrations of AsO_4^{3-} and AsO_4^{3-} + Fe_2O_3-NPs treatments, are significantly different at $P < 0.05$.

then rinsed with sterile distilled water 4–5 times in a laminar flow hood. Fifteen seeds were inoculated in autoclaved glass bottles containing 20 mL test solution. The bottles were incubated in a growth chamber at 25 ± 2 °C under a light intensity of 200-μmol photons m^{-2} s^{-1} (13/11 h light/dark cycle). Two days later, the germinated seedlings were transferred to bottles containing fresh solution. For growth studies, (i) AsO_4^{3-} equivalent to 0.5, 1 and 2 μM; and (ii) Fe_2O_3-NPs equivalent to 100, 200 and 400 mg L^{-1}, were used independently and in combination. However, for further studies, 200 mg L^{-1} Fe_2O_3-NPs were chosen. Respective blanks (without the seeds) were also kept under similar conditions. In a separate set, solutions with equivalent concentrations of $FeCl_3$ were used. However, seeds failed to germinate at equivalent $FeCl_3$ concentrations (alone or in combination with AsO_4^{3-}). Seedlings were harvested after 8 days. Except for SEM investigations, roots of intact seedlings were sonicated for 30–60 s and washed thoroughly with distilled water to remove the Fe_2O_3-NPs attached to the root surface.

2.2.2. Growth analysis

Roots and shoots were separated and washed with distilled water before recording their lengths. For dry biomass measurements, roots and shoots were oven dried at 80 °C to a constant weight.

2.2.3. TEM and SEM analysis

Nanoparticle suspensions in which the seedlings were raised were processed as described in Shabnam et al. (2017). Roots were processed for SEM analysis as described in Shabnam and Kim (2018).

2.2.4. Arsenic and iron content

Roots and shoots were separately assessed for arsenic and iron content. While shoots were directly oven dried at 90 °C, roots were processed to remove any remaining Fe_2O_3-NPs attached to their surface using dithionite-citrate-bicarbonate (DCB) method. Roots were incubated in 30 mL solution consisting of 30 mM sodium citrate, 125 mM sodium bicarbonate and 0.8 g sodium dithionite at 25 °C (Xu and Yu, 2013). After 1 h, roots were washed with distilled water 3–4 times and oven-dried at 90 °C. Dried samples were digested in HNO_3 for 15 min in a BUCHI Digest Automate K-438 (New Castle, DL, USA) at 100 °C. After cooling, the samples were diluted with deionized water. Samples were analyzed for element content using an inductively coupled plasma mass spectrometer (ICP-MS) (Schimadzu ICPE-9000, Kyoto, Japan). To evaluate the dissolution of Fe-ions from Fe_2O_3-NPs and adsorption of AsO_4^{3-} to Fe_2O_3-NPs, respective solutions were ultra-centrifuged at 50,000 × *g* for 30 min. Supernatant was used directly for elemental analysis. To ensure quality control, readings of blank as well as a standard were taken after measurement of every 10 samples.

2.2.5. Ferric chelate reductase activity

Intact seedlings were incubated with their roots immersed in test tubes containing 10 mL assay solution consisting of 10 mM MES (pH 5.5; adjusted using KOH), 0.3mM Ferrozine and 0.1 mM Fe(III)EDTA, at 25 °C in dark (Lucena et al., 2006). After 2 h, roots were excised and weighed. Assay solutions were centrifuged before recording the absorbance at 562 nm for Fe(II)–Ferrozine complex. FCR activity was calculated using an extinction coefficient of 29,8000 M^{-1} cm^{-1} and expressed as nmoles Fe^{2+} g^{-1} fresh weight.

2.2.6. Root oxidising capacity

The protocol of Steponkus and Lanphear (1967) was modified and followed. Briefly, roots were incubated in solution consisting of 0.06% TTC (w/v) in 50 mM Na_2HPO_4–KH_2PO4 buffer (pH 7.4) at 35 °C in dark. After 20 h, roots were washed with distilled water and incubated in 10 mL of 95% ethanol in a water bath for extraction of triphenyl formazan. After cooling, absorbance was recorded at 520 nm. Root oxidisability was expressed as A_{520} h^{-1} g^{-1} fresh weight.

2.2.7. H_2O_2 content

The protocol of Loreto and Velikova (2001) was modified and followed. Samples were homogenised in 5 mL of 0.1% (w/v) TCA containing 2 mM EDTA in a chilled mortar and pestle. Homogenate was centrifuged at 15, 000 × *g* for 15 min at 4 °C. To 1 mL of supernatant, 1 mL each of phosphate buffer (20 mM, pH 7) and potassium iodide (2 M) were added. After 15 min, absorbance of the reaction mixture was recorded at 390 nm. H_2O_2 levels were calculated from a standard curve and expressed as nmoles g^{-1} fresh weight.

2.2.8. Malondialdehyde and proline content

Proline and malondialdehyde (MDA) levels were determined as detailed in Shabnam et al. (2016) and Heath and Packer (1968), respectively.

2.2.9. Total antioxidant capacity

Total antioxidant capacity was determined through measurement of scavenging of DPPH free radical as per the modified protocol of Banerjee et al. (2005). Samples were homogenised in 80% ethanol in a chilled mortar and pestle, centrifuged at 15, 000 × *g* for 20 min at 4 °C. To 0.5 mL supernatant, 2 mL of 95% ethanol and 0.5 mL of 1 mM DPPH (prepared in 95% ethanol) were added and the reaction mixture was kept at 25 ± 2 °C in dark for 30 min. A blank (80% ethanol instead of

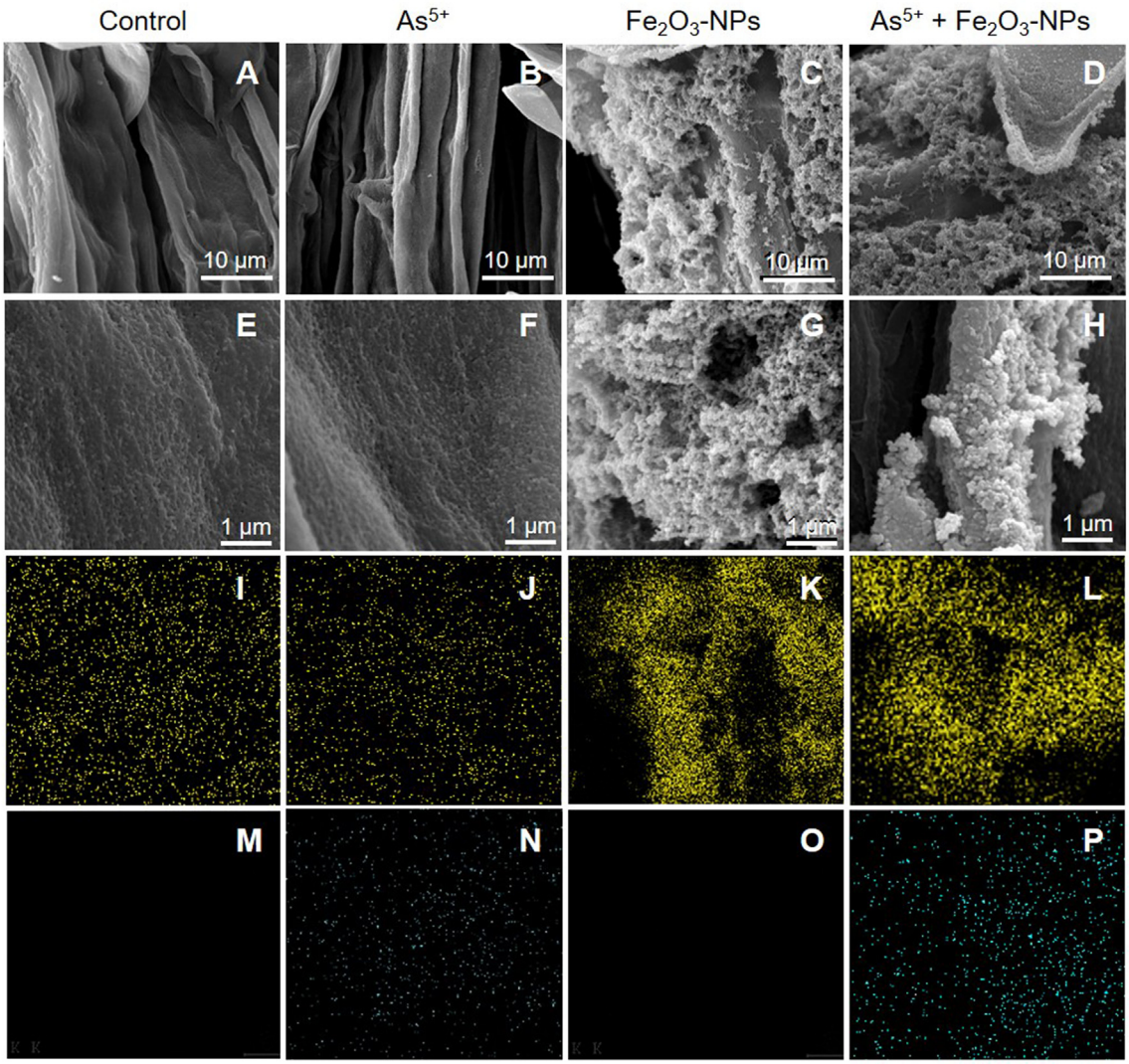

Fig. 5. SEM pictures (A–H) and EDS maps (I–P) for iron (I–L) and arsenic (M–P), of a portion of root surface of *Vigna radiata* seedlings raised in absence (A,E,I,M) and presence of AsO_4^{3-} (B,F,J,N), Fe_2O_3-NPs (C,G,K,O), and AsO_4^{3-} + Fe_2O_3-NPs (D,H,L,P).

sample) was also kept under a similar condition. Absorbance of the reaction mixture was read at 517 nm. DPPH scavenging was calculated by subtracting the absorbance of the sample solution from that of the blank and expressed as nmoles of DPPH scavenged g^{-1} fresh weight using an extinction coefficient of 11,200 M^{-1} cm^{-1} (Sendra et al., 2006).

2.2.10. Antioxidant enzyme activities

Extraction of enzymes and measurement of SOD, CAT and GPX activity were done as described in Shabnam and Kim (2018).

2.2.11. Experimental design and statistical analysis

For each experiment, every treatment had 3 replicates (3 bottles). From each bottle, 4–5 uniform sized plants were used for biochemical analysis. For growth measurements, 10 plants were used from each bottle. All experiments were repeated 5 times. Data are presented as mean ± standard error. Variations between means of AsO_4^{3-} and AsO_4^{3-} + Fe_2O_3-NPs treatments at any single AsO_4^{3-} concentration were determined using Student *t*-test. To determine level of significance between means of different concentrations of AsO_4^{3-} or AsO_4^{3-} + Fe_2O_3-NPs treatments, nested ANOVA was performed followed by Duncan's multiple range test.

3. Results

3.1. Seedling growth

Transmission electron microscope analysis revealed that majority of NPs were ~10–50 nm sized (hexagon)s (Fig. 1). AsO_4^{3-} and Fe_2O_3-NPs, either independently or in combination, did not show any negative effect on seed germination. Contrary to Fe_2O_3-NPs, equivalent concentrations of $FeCl_3$ (independently or in combination with AsO_4^{3-}) caused 100% inhibition in seed germination. A significant decline was noted in length and dry mass of roots of seedlings raised in the presence of AsO_4^{3-} as compared to control (in absence of AsO_4^{3-} and Fe_2O_3-NPs). However, shoots showed only a minor decline in growth. The length and dry biomass of shoots reduced by ~8% and ~12% in the presence of 2 μM AsO_4^{3-}, respectively (Fig. 2B,D). Fe_2O_3-NPs showed a significant increase (~11%) in dry mass of the seedlings (Fig. 2B,D). Interestingly, AsO_4^{3-}-induced decline in seedling growth was not observed in the presence of Fe_2O_3-NPs. For example, a 75% decline in the root length caused by 2 μM AsO_4^{3-} was brought down to 20% by 100 mg L^{-1} Fe_2O_3-NPs (Fig. 2A). Similarly, a 60% decline in the dry biomass of roots induced by 2 μM AsO_4^{3-} reduced to ~15% in the presence of 100 mg L^{-1} Fe_2O_3-NPs (Fig. 2B). A complete recovery was noted in the AsO_4^{3-}-induced negative seedling growth in the presence of

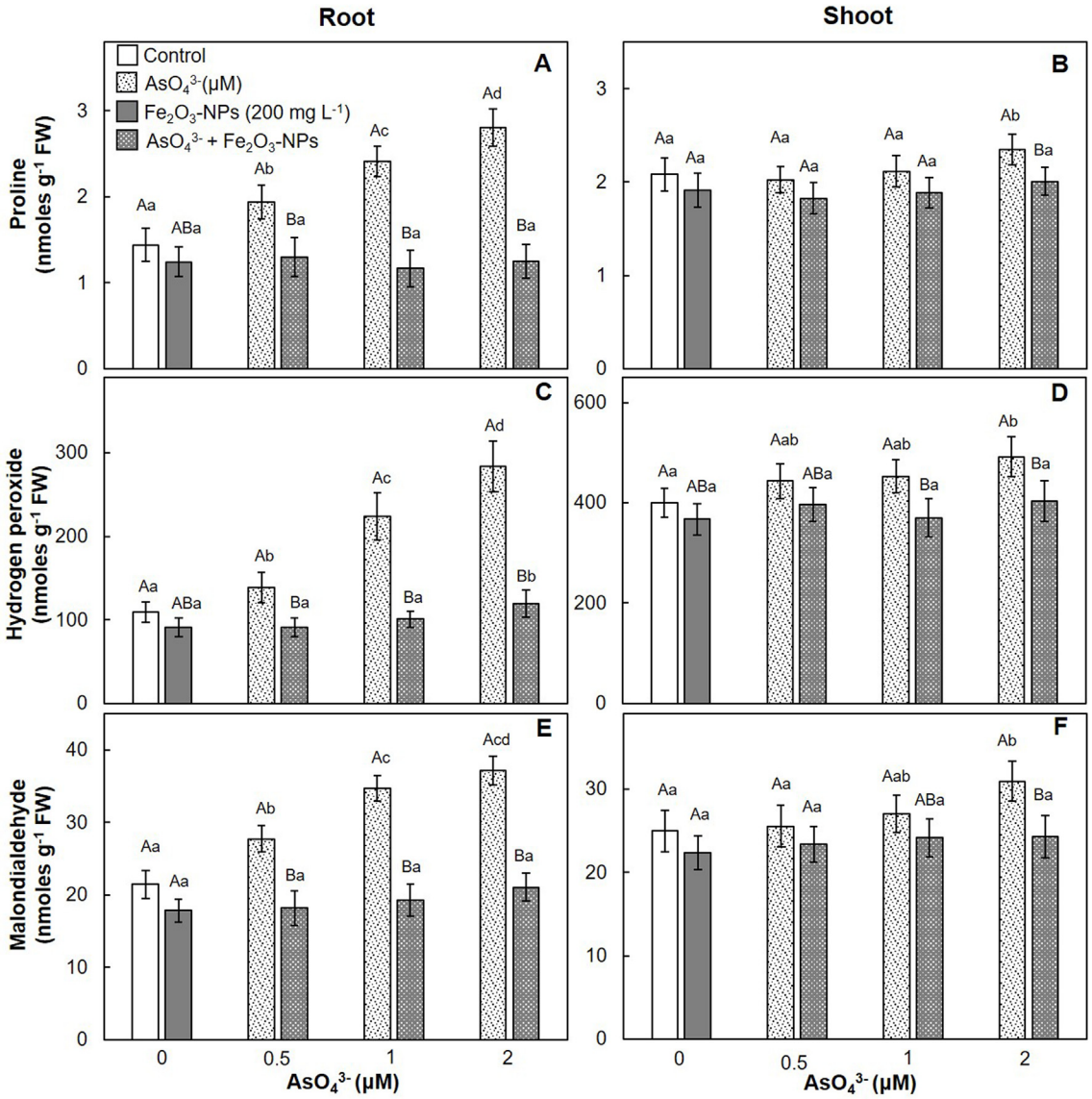

Fig. 6. Impact of Fe_2O_3-NPs on AsO_4^{3-}-induced changes in proline (A,B), H_2O_2 (C,D) and malondialdehyde (E,F) content in roots (A,C,E) and shoots (B,D,F) of *Vigna radiata* seedlings. Vertical lines on bars represent standard error. Values designated by (i) different capital letters between AsO_4^{3-} and AsO_4^{3-} + Fe_2O_3-NPs treatments at a given AsO_4^{3-} concentration; and (ii) small letters between varying concentrations of AsO_4^{3-} and AsO_4^{3-} + Fe_2O_3-NPs treatments, are significantly different at $P < 0.05$.

Fe_2O_3-NPs equivalent to 200 and 400 mg L^{-1}.

3.2. Arsenic and iron content of seedlings

Arsenic levels in seedlings increased significantly with AsO_4^{3-} concentrations in which they were raised (Fig. 3A and B). Arsenic content was higher in roots over shoots. For e.g., at the highest AsO_4^{3-} concentration (i.e., 2 μM), arsenic contents in roots and shoots of seedlings were ~30 and 10 folds higher than those of the respective controls (Fig. 3A and B). Arsenic content was significantly lower in seedlings raised in the presence of both AsO_4^{3-} and Fe_2O_3-NPs. Roots and shoots of seedlings raised in 2 μM AsO_4^{3-} in the presence of Fe_2O_3-NPs showed ~16 and ~5 folds lower arsenic levels, respectively, than those grown in absence of Fe_2O_3-NPs (Fig. 3A and B). Seedlings raised in Fe_2O_3-NPs, in the absence and presence of AsO_4^{3-}, showed significantly higher Fe levels (~2 folds) compared to those of the respective controls (Fig. 3C and D).

3.3. Root-associated activities of seedlings

The root FCR activity of seedlings raised in AsO_4^{3-} increased in a concentration dependent manner (Fig. 4A). This increase in the root FCR activity was curtailed by Fe_2O_3-NPs. For e.g., the FCR activity on exposure to 2 μM AsO_4^{3-}, in the absence and presence of Fe_2O_3-NPs, was ~29.7 and 10 nmoles Fe^{2+} g^{-1} fresh weight, respectively. Interestingly, the root FCR activity of seedlings raised in Fe_2O_3-NPs, in absence or presence of AsO_4^{3-}, was lower than that of the control (Fig. 4A). In contrast to FCR activity, the root oxidising capacity of the seedlings decreased with AsO_4^{3-} concentrations. The decrease was over 50% in roots of the seedlings raised in 2 μM AsO_4^{3-} (Fig. 4B). No change was recorded in roots of the seedlings raised in Fe_2O_3-NPs, in the absence or presence of AsO_4^{3-}, compared to control (Fig. 4B).

3.4. Root surface structure of seedlings

No alterations were recorded on the root-surface structure of the seedlings raised in the presence of AsO_4^{3-} compared to the control

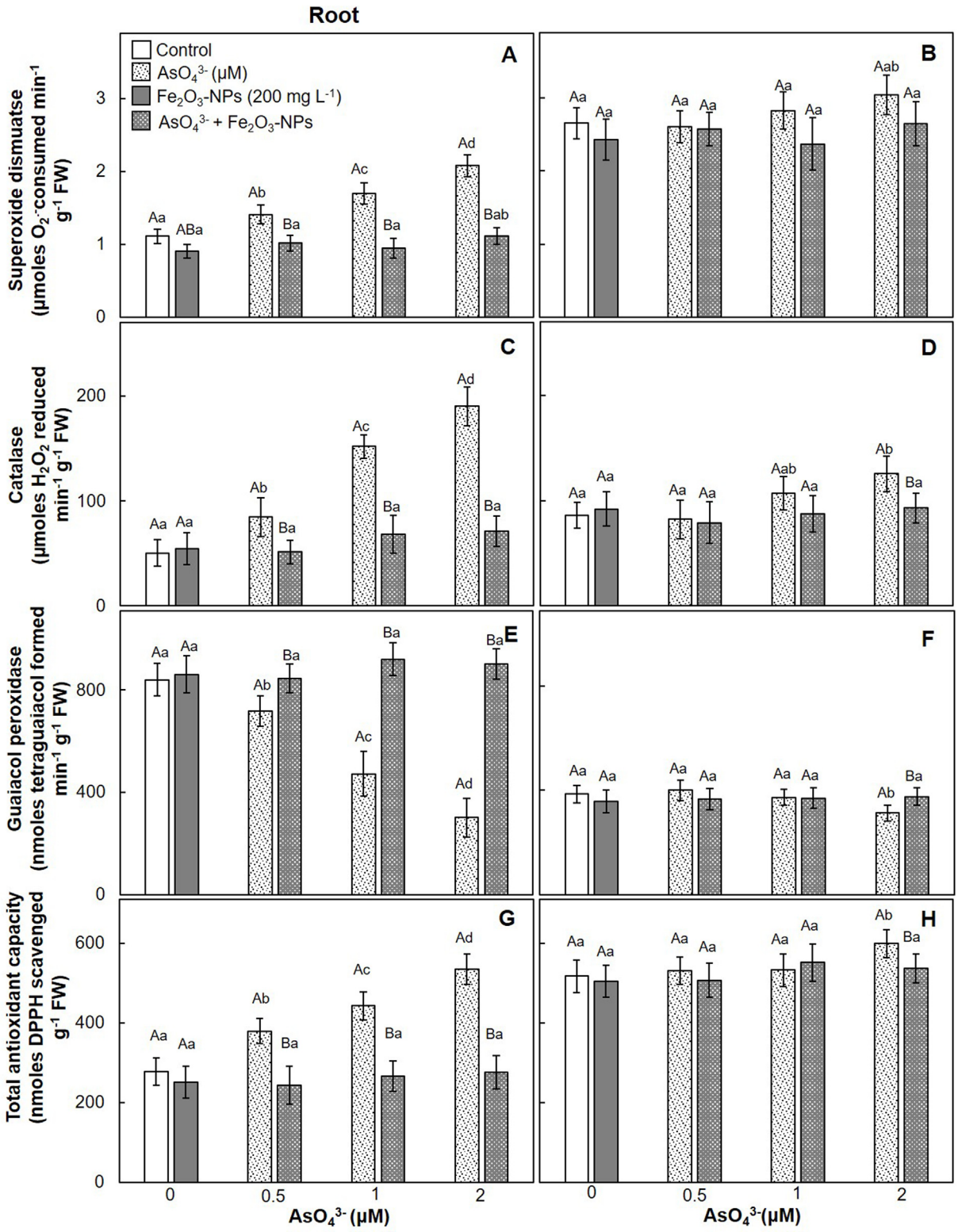

Fig. 7. Impact of Fe_2O_3-NPs on AsO_4^{3-}-induced changes on SOD (A,B), CAT (C,D) and GPX (E,F) activities; and total antioxidant capacity (G,H) in roots (A,C,E,G) and shoots (B,D,F,H) of *Vigna radiata* seedlings. Vertical lines on bars represent standard error. Values designated by (i) different capital letters between AsO_4^{3-} and AsO_4^{3-} + Fe_2O_3-NPs treatments at a given AsO_4^{3-} concentration; and (ii) small letters between varying concentrations of AsO_4^{3-} and AsO_4^{3-} + Fe_2O_3-NPs treatments, are significantly different at $P < 0.05$.

(Fig. 5A,B,E,F). The EDS investigations showed presence of arsenic on the root surface of seedlings raised in the presence of AsO_4^{3-} (Fig. 5N). Distinct NPs/nanocomplexes were detected on the root surface of seedlings raised in the presence of Fe_2O_3-NPs; these complexes were composed of Fe (Fig. 5C,G,K). Roots of the seedlings raised in the presence of AsO_4^{3-} and Fe_2O_3-NPs were also noted with presence of NPs/nanocomplexes which were composed of both Fe and As (Fig. 5D,H,P).

3.5. Oxidative stress in seedlings

While proline levels in the shoots of the seedlings raised in the presence of AsO_4^{3-} showed little to no alteration, the same in the roots increased significantly with AsO_4^{3-} concentrations (Fig. 6A and B). Proline content in roots of the seedlings raised in 2 μM AsO_4^{3-} was ~2 times higher than the control. AsO_4^{3-}-induced increase in proline levels were brought down significantly in the seedlings raised in the presence of Fe_2O_3-NPs; proline levels in these seedlings were similar to that in the control (Fig. 6A and B). The seedlings raised in Fe_2O_3-NPs did not show any alteration in proline levels (Fig. 6A and B). Levels of H_2O_2 also increased in the seedlings raised in AsO_4^{3-}, the increase being prominent in roots over shoots (Fig. 6C and D). H_2O_2 levels in the roots and shoots of the seedlings raised in 2 μM AsO_4^{3-} was ~1.8 and 1.2 folds higher than the respective controls. AsO_4^{3-}-induced increase in H_2O_2 levels were significantly curtailed by Fe_2O_3-NPs. For e.g., H_2O_2 content of seedlings raised in 2 μM AsO_4^{3-} in presence of Fe_2O_3-NPs showed an increase of only 1.2 fold over control (Fig. 6C and D). No difference was recorded in H_2O_2 levels between control and those raised in presence of Fe_2O_3-NPs alone. A similar trend was noted for MDA levels in the seedlings. MDA content increased in the seedlings raised in AsO_4^{3-} where the change was more pronounced in roots than shoots (Fig. 6E and F). For example, while roots of the seedlings raised in 2 μM AsO_4^{3-} showed a 2.8-fold increase, shoots showed ~1.2 fold increase compared to the respective controls. Such increase in MDA levels was not recorded in the seedlings raised in AsO_4^{3-} in the presence of Fe_2O_3-NPs. No alterations were recorded in MDA levels in the seedlings raised in Fe_2O_3-NPs alone when compared to the control (Fig. 6E and F).

AsO_4^{3-} caused significant changes in activity of SOD, CAT and GPX in the seedlings raised in AsO_4^{3-}, the changes being prominent in roots than in shoots. While the SOD and CAT activities were enhanced in roots in response to AsO_4^{3-}, the GPX activity showed a significant decline, compared to respective controls (Fig. 7A–F). AsO_4^{3-}-induced changes in enzyme activities were significantly recovered by Fe_2O_3-NPs. In the case of the SOD activity, the increase of ~1.9 fold induced by 2 μM AsO_4^{3-} in roots was brought down to the level similar to that of the control by Fe_2O_3-NPs (Fig. 7A and B). Activity of CAT in roots of the seedlings raised in 2 μM AsO_4^{3-}, in absence and presence of Fe_2O_3-NPs, was ~3.8 and 1.4 times higher than the control, respectively (Fig. 7C and D). In the case of GPX, the activity declined by over 60% in roots of seedlings exposed to 2 μM AsO_4^{3-} which was 100% recovered by Fe_2O_3-NPs (Fig. 7E and F). No alterations were recorded in the activities of these enzymes in the seedlings raised in Fe_2O_3-NPs alone, when compared to control (Fig. 7A–F). Total antioxidant capacity of the seedlings was significantly enhanced in response to AsO_4^{3-}. In roots, the DPPH-scavenging capacity increased with the AsO_4^{3-} concentrations (Fig. 7G and H). However, in the case of shoots, a significant increase was noted only at 2 μM AsO_4^{3-} which was ~1.15 times higher than the control. Again, AsO_4^{3-} induced increase in the DPPH-scavenging capacity was curtailed significantly by Fe_2O_3-NPs. An increase of ~1.9 folds in the DPPH-scavenging capacity of roots in response to 2 μM AsO_4^{3-} was brought down to ~1.15 folds by Fe_2O_3-NPs. No change was noted in the DPPPH-scavenging capacity of the seedlings raised in Fe_2O_3-NPs alone.

4. Discussion

4.1. Fe_2O_3-NPs curtail AsO_4^{3-}-induced negative seedling growth

While seed germination was unaffected by Fe_2O_3-NPs, it was completely inhibited by $FeCl_3$. This revealed that the nanoparticulate form of Fe is less toxic than the ionic form. AsO_4^{3-} drastically reduced the seedling growth, the decline being stronger in roots than shoots thus resulting in a decreased root to shoot ratio. These results are in accordance with the previous reports on arsenic toxicity in various plants including *V. radiata* (Shri et al., 2009; Singh et al., 2009; Malik et al., 2012; Praveen et al., 2018). AsO_4^{3-} is structurally a chemical analog of phosphate and is taken up by plants via phosphate transporters (Abedin et al., 2002; Farooq et al., 2016). Fe_2O_3-NPs (in the absence of AsO_4^{3-}) had a slightly positive effect on the seedling growth. Positive effects of Fe-based NPs on plant growth (increased biomass) has been reported for *Citrullus lanatus, Pisum sativum*, *Brassica juncea* and *Oryza sativa* (Singh et al., 2009; Li et al., 2013; Huang et al., 2018; Rui et al., 2016). However, there are also reports of toxic and/or non-toxic effects of Fe oxide NPs on plants like Bt. Cotton, *Cucurbita maxima*, *Arabidopsis thaliana* (Zhu et al., 2008; Lee et al., 2010; Van Nhan et al., 2016). The exact reasons behind such varied response of Fe-based NPs remain conflicted and should be explored more. AsO_4^{3-}-induced reduction in seedling growth was not observed in the presence of Fe_2O_3-NPs. A complete recovery was obtained by Fe_2O_3-NPs equivalent to 200 and 400 mg L^{-1}, where the seedling growth was similar to that of the control. The drastic reduction in the seedling growth can be attributed to the uptake of arsenic. Reduction in the seedling growth was directly proportional to the amount of arsenic taken up by the seedlings. This is further established by the fact that the uptake of arsenic was higher in roots than shoots, thus, resulting in a stronger negative effect on the root growth. Reduction in the seedling growth of *V. radiata* induced by arsenic accumulation is in line with the previously published works on arsenic toxicity (Shri et al., 2009; Malik et al., 2012). Higher iron content in the seedlings raised in Fe_2O_3-NPs (in absence or presence of AsO_4^{3-}) can be attributed to a significant release of Fe ions from Fe_2O_3-NPs in the suspensions. In this study, a suspension of 200 mg L^{-1} Fe_2O_3-NPs released ~450 μg L^{-1} of ionic Fe (Supplementary information 1). Previous studies have also reported the release of metal ions from solutions containing metal NPs (Malvindi et al., 2014; Shukla et al., 2015). However, in this study, the Fe levels taken up by the seedlings were not toxic to their growth.

4.2. Fe_2O_3-NPs reduce arsenic bioavailability

Lower arsenic content in the seedlings raised in both AsO_4^{3-} and Fe_2O_3-NPs compared to those raised in only AsO_4^{3-}, signifies the role of Fe_2O_3-NPs in restricting arsenic uptake by seedlings. Previous studies have shown the efficiency of Fe_2O_3-NPs in sorption of arsenic. In this study, EDS of the Fe_2O_3-NPs (in which seedlings were raised in presence of AsO_4^{3-}) showed arsenic specific peaks which revealed that AsO_4^{3-} was successfully absorbed/adsorbed on Fe_2O_3-NPs. AsO_4^{3-} did not cause any deformity on the root surface of seedlings as revealed by SEM studies. This is contradictory to a study in which AsO_4^{3-} exposure (100 μM) caused major alterations in the root-surface structure of rice (Nath et al., 2014). SEM studies also revealed that Fe_2O_3-NPs were restricted to the root surface of seedlings. This could be one of the reasons behind non-toxicity of Fe_2O_3-NPs on the seedling growth. EDS analysis of Fe_2O_3-NPs on the root surface of the seedlings raised in AsO_4^{3-} in the presence of Fe_2O_3-NPs showed the presence of arsenic. This explains that AsO_4^{3-} was absorbed/adsorbed by Fe_2O_3-NPs, thus reducing its availability at the root surface. Hence, it can be concluded that AsO_4^{3-} availability to seedlings is reduced by (i) adsorption of AsO_4^{3} by Fe_2O_3-NPs in the suspension in which seedlings were raised; and/or (ii) adsorption of AsO_4^{3} by Fe_2O_3-NPs that are adhered to the root surface.

As discussed in the above section, a significant amount of Fe ions was released from Fe_2O_3-NPs in the solution resulting in higher Fe levels in the seedlings raised in Fe_2O_3-NPs (supplementary information 1). One among various strategies evolved by plant roots to uptake Fe is the reduction of Fe^{3+} to Fe^{2+} by the plasma-membrane-embedded ferric chelate reductase (FCR), Fe^{2+} is then taken up by Fe(II) transporter proteins (Waters et al., 2002; Hell and Stephan, 2003). The root FCR activity was lower in the seedlings raised in Fe_2O_3-NPs than that of the control. Fe deficiency is a well-known cause to induce the FCR activity as well as upregulate the associated genes. As a result, FCR

activity was higher in control seedlings since they were raised in distilled water without any Fe source, and those raised in Fe_2O_3-NPs were exposed to Fe ions released from Fe_2O_3-NPs. Interestingly, FCR activity was enhanced in response to AsO_4^{3-}; a similar increase has also been reported in various plant species in response to heavy metals (Chang et al., 2003; Lešková et al., 2017; Bari et al., 2019). It was concluded by these researchers that enhanced FCR activity was a result of Fe-deficiency induced by the heavy metals. However, in our study no significant changes were recorded in Fe levels in roots of the seedlings raised in AsO_4^{3-}. However, Fe_2O_3-NPs brought down AsO_4^{3-} stress enhanced FCR activity, thus affirming their role in protecting roots of the seedlings against AsO_4^{3-} stress. At present, we do not have any clear explanation behind the AsO_4^{3-}-induced enhancement in the FCR activity, and further research needs to be done for addressing this phenomenon. Roots of the seedlings raised in AsO_4^{3-} showed a drastic reduction in their oxidisability, which is similar to earlier reports (Malik et al., 2012). However, AsO_4^{3-}-induced decline in root oxidisability was overcome by Fe_2O_3-NPs. Reduction of TTC (or rood oxidisability) is a measure of cell viability and dehydrogenase activity (Hawrylak-Nowak et al., 2015). Our findings indicate the role of Fe_2O_3-NPs in restoring the cell viability and dehydrogenase activity in AsO_4^{3-} exposed roots. Root oxidisability is often directly associated with the ability to reduce the uptake of toxicants (Singh et al., 2009). Recovery of the root oxidisability by Fe_2O_3-NPs further points towards their role in reducing the uptake of arsenic by roots.

4.3. *Fe_2O_3-NPs antagonise AsO_4^{3}-induced oxidative stress*

AsO_4^{3-} is well documented to imbalance redox homeostasis in plants. Similar to earlier reports, the levels of proline (an amino acid), H_2O_2 (an ROS) and MDA (a product of lipid peroxidation) were enhanced in roots of the seedlings raised in AsO_4^{3-}. The increase in levels of these molecules was curtailed by Fe_2O_3-NPs. Proline maintains the NAD(P)H/NAD(P)$^+$ ratio to prevent the formation of ROS and also acts as a quencher of ROS (Shabnam et al., 2016). H_2O_2 is among the most abundant ROS in plants and its levels spike up during an oxidative stress, resulting in disrupted cellular functions and membrane damage through lipid peroxidation (Singh et al., 2009). Curtailment of proline, H_2O_2 and MDA levels by Fe_2O_3-NPs in AsO_4^{3-}-exposed seedlings establish the role of Fe_2O_3-NPs in protecting the seedlings against the AsO_4^{3-}-induced oxidative stress. Levels of H_2O_2 depend on a complex interplay between its production and scavenging by various enzymes. SOD converts highly toxic superoxide anion radicals to less toxic H_2O_2 (Shri et al., 2009; Singh et al., 2009; Shabnam et al., 2017). AsO_4^{3-} exposure resulted in enhanced SOD activity in roots which could largely be responsible for high H_2O_2 levels. Plants have evolved various enzymatic means to get rid of toxic levels of H_2O_2. Activity of CAT, a prominent enzyme which reduces H_2O_2 to water (Shri et al., 2009; Singh et al., 2009; Shabnam et al., 2017), was escalated by AsO_4^{3-}. Another important H_2O_2 detoxification enzyme is GPX which uses phenol compounds as a donor to detoxify H_2O_2 (Shabnam et al., 2017). Contrary to CAT, the activity of GPX declined in the presence of AsO_4^{3-}. Such changes in these enzyme activities in response to AsO_4^{3-} have been reported earlier (Singh et al., 2009; Malik et al., 2012; Praveen et al., 2018). AsO_4^{3-}-induced changes in the activity of these enzymes were retrieved to control levels by Fe_2O_3-NPs. Total antioxidant capacity of the roots of seedlings (evaluated through reduction of DPPH radical) was also enhanced by AsO_4^{3-} which was brought back to control levels by Fe_2O_3-NPs. In summary, our findings furnish the evidence that Fe_2O_3-NPs antagonise the oxidative stress induced by AsO_4^{3-} toxicity in *V. radiata* seedlings.

5. Conclusions

Our findings clearly demonstrated that Fe_2O_3-NPs provide resistance against AsO_4^{3-}-induced toxicity on early seedling growth of *V. radiata*. The AsO_4^{3-}-induced oxidative stress in the seedlings was ameliorated by Fe_2O_3-NPs. The ameliorative effects of Fe_2O_3-NPs are credited to the adsorption of AsO_4^{3-} by Fe_2O_3-NPs which reduced the availability of AsO_4^{3-} to seedlings thus resulting in lower uptake of arsenic. Moreover, Fe_2O_3-NPs did not impose any negative effect on the seedling growth due to their restriction to the root surface, resulting in non-toxic levels of Fe in the seedlings. Our findings furnish a prospect for the use of Fe-oxide and/or Fe-based NPs to reduce/minimise AsO_4^{3-}-toxicity in plants under field conditions. However, further research needs to be done in this aspect.

Acknowledgments

We appreciate help of Prof. Sun-Hyung Kim, Department of Horticulture, University of Seoul, for ultracentrifuge facilities. This research was funded by Ministry of Agriculture, Food and Rural affairs, Korea Govt. (Project No.- PJ014352042019).

Appendix A. Supplementary data

Supplementary data to this article can be found online at https://doi.org/10.1016/j.ecoenv.2019.109496.

References

Abedin, M.J., Feldmann, J., Meharg, A.A., 2002. Uptake kinetics of arsenic species in rice plants. Plant Physiol. 128, 1120–1128.
Ali, A., Hira Zafar, M.Z., ul Haq, I., Phull, A.R., Ali, J.S., Hussain, A., 2016. Synthesis, characterization, applications, and challenges of iron oxide nanoparticles. Nanotechnol. Sci. Appl. 9, 49–67.
Banerjee, A., Dasgupta, N., De, B., 2005. In vitro study of antioxidant activity of *Syzygium cumini* fruit. Food Chem. 90, 727–733.
Bari, M.A., Akther, M.S., Reza, M.A., Kabir, A.H., 2019. Cadmium tolerance is associated with the root-driven coordination of cadmium sequestration, iron regulation, and ROS scavenging in rice. Plant Physiol. Biochem. 136, 22–33.
Bezbaruah, A.N., Krajangpan, S., Chisholm, B.J., Khan, E., Bermudez, J.J.E., 2009. Entrapment of iron nanoparticles in calcium alginate beads for groundwater remediation applications. J. Hazard Mater. 166, 1339–1343.
Chang, Y.C., Zouari, M., Gogorcena, Y., Lucena, J.J., Abadía, J., 2003. Effects of cadmium and lead on ferric chelate reductase activities in sugar beet roots. Plant Physiol. Biochem. 41, 999–1005.
Crane, R.A., Scott, T.B., 2012. Nanoscale zero-valent iron: future prospects for an emerging water treatment technology. J. Hazard Mater. 211, 112–125.
Cundy, A.B., Hopkinson, L., Whitby, R.L., 2008. Use of iron-based technologies in contaminated land and groundwater remediation: a review. Sci. Total Environ. 400, 42–51.
Duncan, E.G., Maher, W.A., Foster, S.D., Krikowa, F., O'Sullivan, C.A., Roper, M.M., 2017. Dimethylarsenate (DMA) exposure influences germination rates, arsenic uptake and arsenic species formation in wheat. Chemosphere 181, 44–54.
Farooq, M.A., Islam, F., Ali, B., Najeeb, U., Mao, B., Gill, R.A., Yan, G., Siddique, K.H., Zhou, W., 2016. Arsenic toxicity in plants: cellular and molecular mechanisms of its transport and metabolism. Environ. Exp. Bot. 132, 42–52.
Hartley, W., Lepp, N.W., 2008. Remediation of arsenic contaminated soils by iron-oxide application, evaluated in terms of plant productivity, arsenic and phytotoxic metal uptake. Sci. Total Environ. 390, 35–44.
Hawrylak-Nowak, B., Dresler, S., Matraszek, R., 2015. Exogenous malic and acetic acids reduce cadmium phytotoxicity and enhance cadmium accumulation in roots of sunflower plants. Plant Physiol. Biochem. 94, 225–234.
Heath, R.L., Packer, L., 1968. Photoperoxidation in isolated chloroplast. I. Kinetics and stoichiometry of fatty acid peroxidation. Arch. Biochem. Biophys. 125, 189–198.
Hell, R., Stephan, U.W., 2003. Iron uptake, trafficking and homeostasis in plants. Planta 216, 541–551.
Hokkanen, S., Repo, E., Lou, S., Sillanpää, M., 2015. Removal of arsenic (V) by magnetic nanoparticle activated microfibrillated cellulose. Chem. Eng. J. 260, 886–894.
Hu, X., Zhang, Y., Ding, Z., Wang, T., Lian, H., Sun, Y., Wu, J., 2012. Bioaccessibility and health risk of arsenic and heavy metals (Cd, Co, Cr, Cu, Ni, Pb, Zn and Mn) in TSP and PM 2. 5 in Nanjing, China. Atmosph. Environ. Times 57, 146–152.
Huang, Q., Liu, Q., Lin, L., Li, F.J., Han, Y., Song, Z.G., 2018. Reduction of arsenic toxicity in two rice cultivar seedlings by different nanoparticles. Ecotoxicol. Environ. Saf. 159, 261–271.
Jang, M., Chen, W., Cannon, F.S., 2008. Preloading hydrous ferric oxide into granular activated carbon for arsenic removal. Environ. Sci. Technol. 42, 3369–3374.
Kumpiene, J., Ore, S., Renella, G., Mench, M., Lagerkvist, A., Maurice, C., 2006. Assessment of zerovalent iron for stabilization of chromium, copper, and arsenic in soil. Environ. Pol. 144, 62–69.
Lee, C.W., Mahendra, S., Zodrow, K., Li, D., Tsai, Y.C., Braam, J., Alvarez, P.J., 2010. Developmental phytotoxicity of metal oxide nanoparticles to *Arabidopsis thaliana*. Environ. Toxicol. Chem. 29, 669–675.

Lenoble, V., Laclautre, C., Deluchat, V., Serpaud, B., Bollinger, J.C., 2005. Arsenic removal by adsorption on iron (III) phosphate. J. Hazard Mater. 123, 262–268.
Lešková, A., Giehl, R.F., Hartmann, A., Fargašová, A., von Wirén, N., 2017. Heavy metals induce iron deficiency responses at different hierarchic and regulatory levels. Plant Physiol. 174, 1648–1668.
Li, J., Chang, P.R., Huang, J., Wang, Y., Yuan, H., Ren, H., 2013. Physiological effects of magnetic iron oxide nanoparticles towards watermelon. J. Nanosci. Nanotechnol. 13, 5561–5567.
Loreto, F., Velikova, I.V., 2001. Isoprene produced by leave s protect the photosynthetic apparatus against ozone damage, quenches ozone products, and reduces lipid peroxidation of cellular membranes. Plant Physiol. 127, 1781–1787.
Lucena, C., Waters, B.M., Romera, F.J., García, M.J., Morales, M., Alcántara, E., Pérez-Vicente, R., 2006. Ethylene could influence ferric reductase, iron transporter, and H +-ATPase gene expression by affecting FER (or FER-like) gene activity. J. Exp. Bot. 57, 4145–4154.
Malik, J.A., Goel, S., Kaur, N., Sharma, S., Singh, I., Nayyar, H., 2012. Selenium antagonises the toxic effects of arsenic on mungbean (*Phaseolus aureus Roxb*.) plants by restricting its uptake and enhancing the antioxidative and detoxification mechanisms. Environ. Exp. Bot. 77, 242–248.
Malvindi, M.A., De Matteis, V., Galeone, A., Brunetti, V., Anyfantis, G.C., Athanassiou, A., Cingolani, R., Pompa, P.P., 2014. Toxicity assessment of silica coated iron oxide nanoparticles and biocompatibility improvement by surface engineering. PLoS One 9, e85835.
Meharg, A.A., 2004. Arsenic in rice–understanding a new disaster for South-East Asia. Trends Plant Sci. 9, 415–417.
Mench, M., Vangronsveld, J., Beckx, C., Ruttens, A., 2006. Progress in assisted natural remediation of an arsenic contaminated agricultural soil. Environ. Pollut. 144, 51–61.
Nath, S., Panda, P., Mishra, S., Dey, M., Choudhury, S., Sahoo, L., Panda, S.K., 2014. Arsenic stress in rice: redox consequences and regulation by iron. Plant Physiol. Biochem. 80, 203–210.
Praveen, A., Khan, E., Perwez, M., Sardar, M., Gupta, M., 2018. Iron oxide nanoparticles as nano-adsorbents: a possible way to reduce arsenic phytotoxicity in Indian mustard plant (*Brassica juncea* L.). J. Plant Growth Regul. 37, 612–624.
Rui, M., Ma, C., Hao, Y., Guo, J., Rui, Y., Tang, X., Zhao, Q., Fan, X., Zhang, Z., Hou, T., Zhu, S., 2016. Iron oxide nanoparticles as a potential iron fertilizer for peanut (*Arachis hypogaea*). Front. Plant Sci. 7, 815.
Sendra, J.M., Sentandreu, E., Navarro, J.L., 2006. Reduction kinetics of the free stable radical 2,2-diphenyl-1-picrylhydrazyl (DPPH•) for determination of the antiradical activity of citrus juices. Eur. Food Res. Technol. 223, 615–624.
Shabnam, N., Kim, H., 2018. Non-toxicity of nano alumina: a case on mung bean seedlings. Ecotoxicol. Environ. Saf. 165, 423–433.
Shabnam, N., Sharmila, P., Kim, H., Pardha-Saradhi, P., 2017. Differential response of floating and submerged leaves of long leaf pondweed, *Potamogeton nodosus*, to silver ions. Front. Plant Sci. 8, 1052.
Shabnam, N., Tripathi, I., Sharmila, P., Pardha-Saradhi, P., 2016. A rapid, ideal and ecofriendlier protocol for quantifying proline. Protoplasma 253, 1577–1582.
Shipley, H.J., Engates, K.E., Guettner, A.M., 2011. Study of iron oxide nanoparticles in soil for remediation of arsenic. J. Nanoparticle Res. 13, 2387–2397.
Shri, M., Kumar, S., Chakrabarty, D., Trivedi, P.K., Mallick, S., Misra, P., Shukla, D., Mishra, S., Srivastava, S., Tripathi, R.D., Tuli, R., 2009. Effect of arsenic on growth, oxidative stress, and antioxidant system in rice seedlings. Ecotoxicol. Environ. Saf. 72, 1102–1110.
Shukla, S., Jadaun, A., Arora, V., Sinha, R.K., Biyani, N., Jain, V.K., 2015. In vitro toxicity assessment of chitosan oligosaccharide coated iron oxide nanoparticles. Toxicol. Rep. 2, 27–39.
Singh, H.P., Kaur, S., Batish, D.R., Sharma, V.P., Sharma, N., Kohli, R.K., 2009. Nitric oxide alleviates arsenic toxicity by reducing oxidative damage in the roots of Oryza sativa (rice). Nitric Oxide 20, 289–297.
Steponkus, P.L., Lanphear, F.O., 1967. Refinement of the triphenyl tetrazolium chloride method of determining cold injury. Plant Physiol. 2, 1423–1426.
Van Nhan, L., Ma, C., Rui, Y., Cao, W., Deng, Y., Liu, L., Xing, B., 2016. The effects of Fe2O3 nanoparticles on physiology and insecticide activity in non-transgenic and Bt-transgenic cotton. Front. Plant Sci. 6, 1263.
War, A.R., Murugesan, S., Boddepalli, V.N., Srinivasan, R., Nair, R.M., 2017. Mechanism of resistance in Mungbean [Vigna radiata (L.) R. Wilczek var. radiata] to bruchids, Callosobruchus spp. (Coleoptera: Bruchidae). Front. Plant Sci. 8, 1031.
Warren, G.P., Alloway, B.J., Lepp, N.W., Singh, B., Bochereau, F.J.M., Penny, C., 2003. Field trials to assess the uptake of arsenic by vegetables from contaminated soils and soil remediation with iron oxides. Sci. Total Environ. 311, 19–33.
Waters, B.M., Blevins, D.G., Eide, D.J., 2002. Characterization of FRO1, a pea ferric-chelate reductase involved in root iron acquisition. Plant Physiol. 129, 85–94.
Xu, B., Yu, S., 2013. Root iron plaque formation and characteristics under N_2 flushing and its effects on translocation of Zn and Cd in paddy rice seedlings (*Oryza sativa*). Ann. Bot. 111, 1189–1195.
Xu, P., Zeng, G.M., Huang, D.L., Feng, C.L., et al., 2012. Use of iron oxide nanomaterials in wastewater treatment: a review. Sci. Total Environ. 424, 1–10.
Zhu, H., Han, J., Xiao, J.Q., Jin, Y., 2008. Uptake, translocation, and accumulation of manufactured iron oxide nanoparticles by pumpkin plants. J. Environ. Monit. 10, 713–717.
Zou, Y., Wang, X., Khan, A., Wang, P., Liu, Y., Alsaedi, A., Hayat, T., Wang, X., 2016. Environmental remediation and application of nanoscale zero-valent iron and its composites for the removal of heavy metal ions: a review. Environ. Sci. Technol. 50, 7290–7304.